J. Phys. B: At. Mol. Opt. Phys. **22** (1989) 963-970. Printed in the UK

Total cross section measurements for 1–400 eV positrons and electrons in C_2H_2

O Sueoka and S Mori

Institute of Physics, College of Arts and Sciences, University of Tokyo, 3-8-1 Komaba, Meguro-ku, Tokyo 153, Japan

Received 9 August 1988

Abstract. Total cross section (TCS) for 0.7-400 eV positrons and 1-400 eV electrons colliding with acetylene (C_2H_2) molecules are measured using a retarding potential time-of-flight method. The results are compared with those in ethylene (C_2H_4), ethane (C_2H_6) and methane (CH_4) molecules. The effect of the triple bond in C_2H_2 and the double bond in C_2H_4 on the TCS curves is explained by the polarisation interaction. The positronium (Ps) formation corss section is also estimated just above threshold.

1. Introduction

The total cross section (TCS) for electron collisions with C_2H_2 molecules was measured many years ago by Brüche (1929) in the range 1-33 eV, and the TCS for electrons from a multiple-scatting Xα calculation in the range below 5.2 eV has recently been obtained by Tossell (1985). But theoretical data are very much higher than Brüche's experimental data. The differential cross sections for elastic electron scattering in the range 100-1000 eV have been studied experimentally (Fink *et al* 1975) and theoretically (Jain *et al* 1983) using a two-potential coherent approach. On the other hand, no data for positron collisions have yet been presented. In this paper, relative measurements of the TCS for 1-400 eV positrons and electrons scattered by C_2H_2 molecules are performed. The effect of the C-C triple bond in C_2H_2 is discussed by comparison with collision data in hydrocarbons C_2H_4, C_2H_6 and CH_4 (Sueoka and Mori 1986a, hereafter referred to as I). To improve statistics, measurements in e^+-C_2H_4 and e^+-C_2H_6 are performed in the range 1.9-15 eV.

Preliminary data for the TCS for e^+ and e^- using high-purity C_2H_2 gas have already been reported (Sueoka and Mori 1986b, Sueoka 1987).

2. Experimental procedure

The TCS experiments for positron and electron collisions are carried out using a straight absorption-type apparatus using the same experimental procedure as in previous work (Sueoka and Mori 1984, I). A schematic diagram of the experimental set-up is shown in figure 1. A ^{22}Na radioisotope with an activity of 40 μCi and a W-ribbon moderator are used for the source of low-energy positrons. Slow electron beams with energy width of 1.0 eV (FWHM) are composed of secondary electrons produced from the same radioisotope on the emission from the same moderator.

0953-4075/89/060963+08$02.50

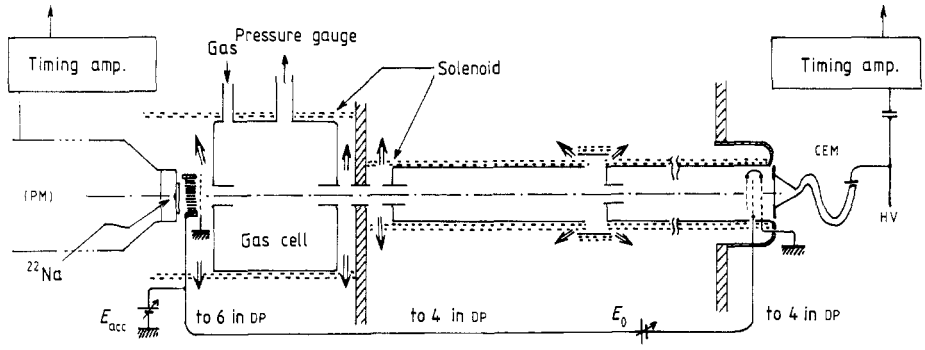

Figure 1. Schematic diagram of the apparatus.

As a spectrometer for e^+ and e^- beams, a time-of-flight (TOF) apparatus with retarding potential is used. The reason why the TCS measurement is possible using a TOF method is the use of a retarding potential method, though the energy width of e^+ and e^- beams is not narrow, and the e^- beam has a long tail on the higher-energy side (I). Namely, the main excitation structures of C_2H_2 by electron impact appear at about 7.6 eV (van Veen and Plantenga 1976). TCS measurements for positrons in C_2H_2 are also possible for the above reason.

A magnetic field produced by solenoids surrounding the collision cell and the flight path is used to transport projectiles. Although the magnetic field in the main part of the flight path is 45 G, in the vicinity of the collision cell a lower magnetic field is used to diminish the contribution of elastic forward scattering. The magnetic field dependence of the TCS for e^+ and e^- beams is determined in the low-energy range. The result for positron collisions is shown in figure 2(*a*). From the apparent cross section values at 0.7–1.0 eV shown in the figure, the TCS for a magnetic field of 3.6 G does not give a saturated value of the TCS versus magnetic field. In the range above 1.6 eV, however, a magnetic field of 4.5 G is of permissible strength, because the TCS curves

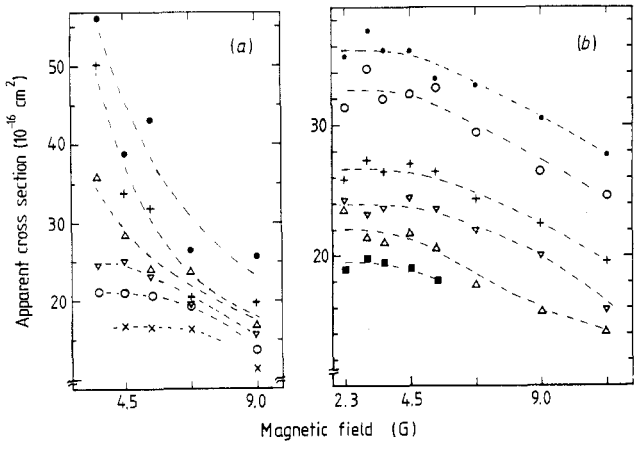

Figure 2. (*a*) Apparent cross sections for positrons plotted against the magnetic field: (●) 0.7 eV, (+) 1.0 eV, (△) 1.3 eV, (▽) 1.6 eV, (○) 2.2 eV and (×) 3.1 eV. Visual fitted curves are shown as a guide. (*b*) Apparent cross sections for electrons plotted against the magnetic field: (■) 1.0 eV, (△) 1.2 eV, (▽) 1.4 eV, (+) 1.6 eV, (○) 2.0 eV and (●) 2.5 eV.

are saturated versus magnetic field. Moreover, in the range above 8.5 eV a magnetic field of 9 G may also be permissible. The magnetic field dependence for electron collisions is shown in figure 2(*b*).

The TCS value, Q_t, is obtained from the equation

$$Q_t = (1/\rho l) \ln(I_v/I_g)$$

where ρ is the density of the collision gas, l is the effective length of the cell, derived by normalisation of the TCS in e^+-N_2 at higher energies (50-400 eV) to the data of Hoffman *et al* (1982)—namely, the TCS values are obtained relatively—and I_v and I_g are net counts subtracted for accidental coincidences in the vacuum and in the gas run. The geometric length of the gas cell is 58.0 mm, but $l = 59.0$ mm assuming the Baratron gauge is correct. The diameters of the two apertures of the cell and that of the holes for differential pumping are 8 mm. As a rough approximation and on the assumption of disregarding the effect of the magnetic field, the systematic error due to forward scattering brought about by elastic scattering is about 4° on average.

High-purity acetylene gas (99.9999%, very expensive) is used for the main measurement; low-purity gas (98.7%) is only used for measurements at lower magnetic field and for the magnetic field dependence, because these measurements take a much longer time. Over the whole measurement, the low-purity gas is used in much higher quantity than the high-purity gas. The main impurities in the low-purity C_2H_2 are N_2 (0.43%), H_2 (0.26%) and CH_4 (0.21%). No distinct effect of the impurities is observed. Namely, the TCS values at 3 G (low-purity gas) and 4.5 G (high-purity gas) coincide with each other within statistical errors (about 1.5%).

To prevent the production of copper acetylide, which is an explosive material, copper parts in the pipe for gas transportation and the flight pipe are used as little as practicable in the low-pressure acetylene gas.

3. Experimental results

The TCS for positrons colliding with C_2H_2 is obtained for magnetic fields of 3.6 G in the range 0.7-2.8 eV, 4.5 G in the range 0.7-10 eV and 9 G in the range 0.7-400 eV. The TCS values are shown in figure 3 together with data for C_2H_4 (obtained by addition of the previous work (I) and new data in the range 2.2-15 eV) and C_2H_6 (obtained by addition of previous data and new data in the range 1.9-11 eV) in the range below 17 eV. As shown in figures 2(*a*) and 3, saturation of the cross section values versus magnetic field at low energies is not shown at these magnetic fields. The true TCS value at 0.7 and 1.0 eV is perhaps higher than the observed values in the 3.6 G measurement. The data for C_2H_4, C_2H_6 and CH_4 in I were measured at 9 G even in the low-energy range. From additional measurements of e^+-C_2H_4 at 4.5 G in the range 2-8 eV, it is deduced that the magnetic field dependence is weak. However, the TCS values for C_2H_4 and CH_4 in the lower-energy range may be somewhat higher for lower magnetic field measurement. Moreover, the results plotted in figures 2(*a*) and 3 for C_2H_2 show that positron scattering in the low-energy range is sharply forward-peaked.

From the TCS curve in figure 3, we cannot directly estimate the positronium (Ps) formation cross section. For such estimation, the TCS values of e^+-C_2H_2 at various magnetic fields are plotted in the inset. As shown there, the Ps formation cross section at just above the threshold energy ($E_{Ps} = 4.6$ eV) of Ps formation is estimated using the cross section curves for higher magnetic field measurements (9 or 23 G). The hatched part in the inset indicates the contribution due to Ps formation. This method

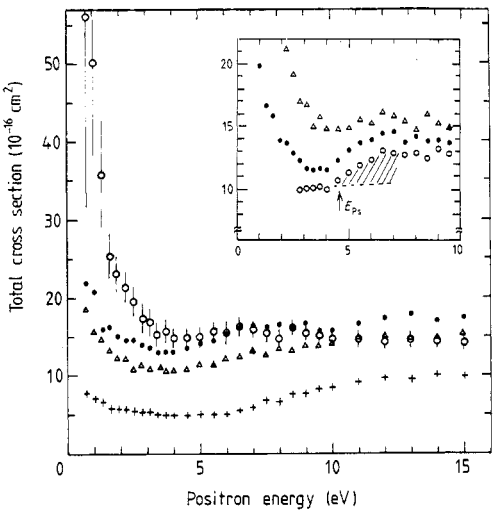

Figure 3. Total cross sections for 0.7–15 eV positrons colliding with C_2H_2 (○), and with C_2H_4 (●), C_2H_6 (△) and CH_4 (+) in I. For the estimation of positronium (Ps) formation, the TCS of e^+-C_2H_2 at 4.5 G (△), 9 G (●) and 23 G (○) are shown in the inset. The broken curve is a guess of the contribution of positron scattering except for Ps formation. Error bars show uncertainties of the present results except the error due to forward scattering. The threshold of Ps formation in C_2H_2 is shown by an arrow.

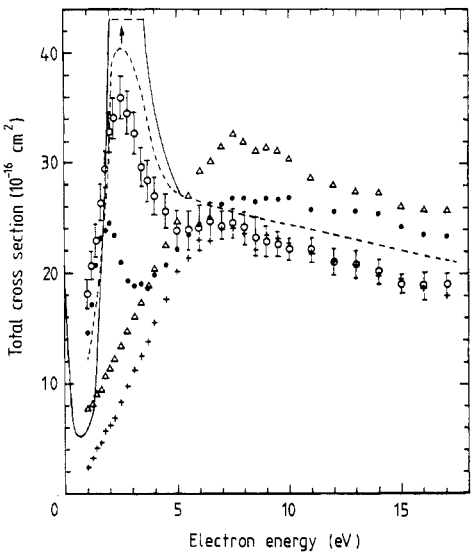

Figure 4. Total cross sections for 1–17 eV electrons with C_2H_2 (○), Brüche's experimental data (— — —) and Tossell's theoretical data (——) in which the shape resonance around the peak (peak value 86×10^{-16} cm^2, peak position 2.6 eV) is not shown. The TCS data in C_2H_4 (●), C_2H_6 (△) and CH_4 (+) are also given (I). Error bars show uncertainties of the present results except the error due to forward scattering.

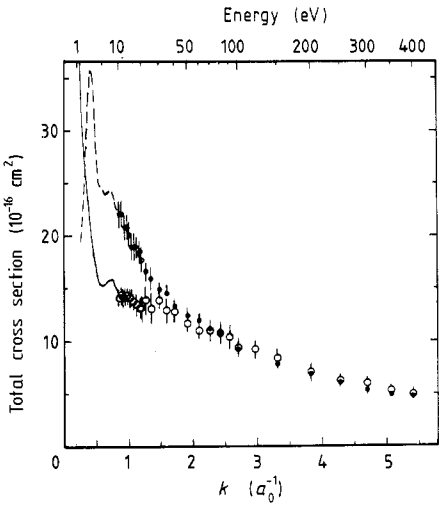

Figure 5. Total cross sections for positrons and electrons against wavenumber k extending to intermediate energies: (○) positrons; (●) electrons. The values in the range below 10 eV are replaced by the full (for e^+) and broken (for e^-) curves, which are the visual fitted curves.

has been previously discussed elsewhere (Sueoka *et al* 1987). The Ps formation cross section, Q_{Ps}, is roughly estimated to be 2.3×10^{-16} cm^2 at 2 eV above E_{Ps}.

The TCS values for electrons colliding with C_2H_4 are measured at 3 G in the range 1.0-6.0 eV and at 4.5 G in the range 1.0-400 eV. The data are presented in figure 4 together with Brüche's experimental data (Brüche 1929), the TCS for electrons from the multiple-scattering X_α calculation of Tossell (1985), and the data for C_2H_4, C_2H_6 and CH_4 in I for comparison. Tossell's theoretical values at the shape resonance are much higher than the experimental data. The 4.5 G data (except at 1.0-1.4 eV) are not affected by the magnetic field. In the range 1.6-6.0 eV, the 4.5 G data and the 3 G data agree well. From the results shown in figures 2(*b*) and 4, the magnetic field dependence of the TCS in electron scattering by C_2H_2 is weak. That is, forward scattering is not dominant even in the low-energy range. The TCS values for electrons are lower than Brüche's data, as shown in CH_4 (I), H_2O and NH_3 (Sueoka *et al* 1987). The 2.4 eV peak in electron scattering due to the shape resonance $^2\Pi_g$ is presented. As the e^- beam in this experiment has a width of 0.6 eV in a direction perpendicular to the flight pipe, the observed resonance peak is not sharp.

The TCS values for positrons and electrons extending to intermediate energies are plotted against wavenumber k in figure 5. The full (positrons) and broken (electrons) curves in the range below 10 eV correspond to the values in figures 3 and 4, respectively. The curve for positron collisions in the range 15-40 eV decreases little with increasing impact energy. The TCS values for e^+ and e^- merge in the intermediate energy range above 100 eV, as shown in the experimental results for hydrocarbons C_2H_4, C_2H_6 and CH_4 (I).

4. Discussion

For positron-atom scattering, the polarisation interaction is subtracted from the static Coulomb interaction. For electron-atom scattering, on the other hand, it is added to

the static Coulomb interaction. In the low-energy region where the polarisation effect is important, the effect of electron–atom scattering is larger than that of positron–atom scattering. From the above fact, the ratio of TCS for positrons to that for electrons, Q_t^+/Q_t^-, is smaller for scattering gases of larger polarisation effect. The results of the ratio may be explained by the distance between the two carbon atoms in the C–C bond (C_2H_2, 1.21 Å; C_2H_4, 1.34 Å; C_2H_6, 1.54 Å) or by the molecular size.

To demonstrate this phenomenon, the ratios for C_2H_2, C_2H_4, C_2H_6 and CH_4 are shown together with the experimental data of Floeder *et al* (1985) for C_2H_4, C_2H_6 and CH_4 in figure 6. The Q_t values used for the ratio should eliminate the contribution of Ps formation, but cases with a contribution are shown in the figure. The low ratios in C_2H_2 and C_2H_4 in the low-energy region are due to the effect of the shape resonance. In the case of elimination of the shape resonance contribution, the ratios (double curves in the figure) have higher values.

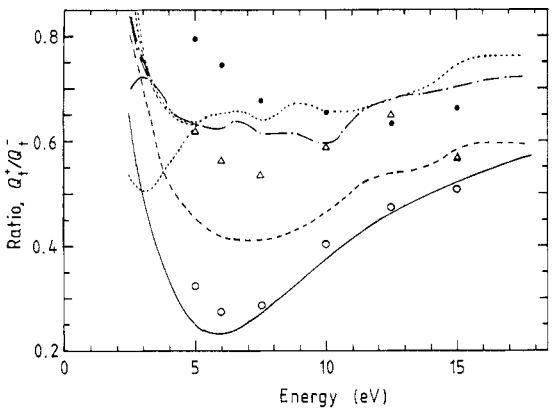

Figure 6. The ratio Q_t^+/Q_t^- of TCS for positrons and electrons plotted against energy (2.5–17 eV). The ratios are replaced by the visual fitted cuves: (· · · ·) C_2H_2, (— · —) C_2H_4, (— — —) C_2H_6 and (——) CH_4. The double dotted and chain curves at the top at low energy are the curves obtained by eliminating the contribution of the shape resonance for e^--C_2H_2 and e^--C_2H_4. The ratios of Floeder *et al* (1985) are given for C_2H_4 (●), C_2H_6 (△) and CH_4 (○).

Although the ratio data involve ambiguity, the next result does follow. The more compact a molecule, the smaller the polarisation effect tends to be. On the other hand, the experimental results also lead to the conclusion that the effect of π-electrons in C_2H_2 and C_2H_4 is not important in the scattering. Meanwhile, the absence of exchange interaction in positron–gas scattering makes the ratio small. But the contribution of exchange interaction does not depend on atomic configuration as much as that of polarisation interaction.

The TCS curve for positrons is rather smooth like all e^+ TCS measurements. That is, a resonance-like structure is not observed. The undefined hump in e^+-C_2H_4 at about 7 eV, which is shown in the previous work (I), seems to shrink in the present data.

The values of TCS for positrons and electrons are given in tables 1 and 2. The error shown is obtained by addition of $\Delta I/I$, $\Delta\rho/\rho$ and $\Delta l/l(=3\%)$, not including the systematic error.

Table 1. Total cross sections for positron collisions (10^{-16} cm^2). The cross section values in the energy range 0.7-1.3 eV are taken from the 3.6 G measurement, those at 1.6-8 eV are taken from the 4.5 G measurement and the others are taken from the 9 G measurement.

Energy (eV)	TCS	Energy (eV)	TCS	Energy (eV)	TCS
0.7	56 ± 25	7.0	15.9 ± 1.1	25.0	13.1 ± 1.4
1.0	50 ± 12	7.5	15.5 ± 1.2	30.0	13.8 ± 0.9
1.3	36 ± 7	8.0	14.8 ± 1.3	35.0	12.9 ± 1.1
1.6	25.2 ± 2.9	8.5	13.9 ± 0.9	40.0	12.8 ± 1.0
1.9	23.0 ± 2.3	9.0	13.9 ± 0.9	50.0	11.7 ± 0.8
2.2	21.2 ± 1.9	9.5	13.7 ± 1.0	60.0	11.0 ± 0.8
2.5	19.2 ± 1.9	10.0	13.5 ± 0.8	70.0	11.0 ± 1.0
2.8	17.1 ± 1.8	11.0	14.5 ± 0.9	80.0	10.8 ± 0.9
3.1	16.8 ± 1.7	12.0	14.2 ± 0.9	90.0	10.4 ± 1.1
3.4	15.0 ± 1.6	13.0	14.3 ± 0.9	100	9.4 ± 0.9
3.7	15.8 ± 1.6	14.0	14.1 ± 0.9	120	9.3 ± 0.9
4.0	14.6 ± 1.2	15.0	14.1 ± 1.0	150	8.3 ± 0.9
4.5	14.9 ± 1.2	16.0	13.8 ± 1.0	200	7.1 ± 0.8
5.0	15.0 ± 1.3	17.0	13.5 ± 1.1	250	6.3 ± 0.6
5.5	15.6 ± 1.3	19.0	13.1 ± 1.1	300	6.0 ± 0.5
6.0	15.3 ± 1.4	20.0	13.3 ± 1.3	350	5.4 ± 0.4
6.5	16.2 ± 1.2	22.0	13.9 ± 1.3	400	5.0 ± 0.5

Table 2. Toatal cross sections for electron collisions (10^{-16} cm^2). The cross section values in the energy range 1.0-6.0 eV are taken from the 3 G measurement and the others are taken from the 4.5 G measurement.

Energy (eV)	TCS	Energy (eV)	TCS	Energy (eV)	TCS
1.0	18.1 ± 1.4	7.0	24.2 ± 1.3	25.0	15.9 ± 1.1
1.2	20.6 ± 1.4	7.5	24.4 ± 1.3	30.0	14.9 ± 0.9
1.4	22.9 ± 1.5	8.0	24.0 ± 1.4	35.0	14.6 ± 0.9
1.6	26.3 ± 1.7	8.5	23.1 ± 1.6	40.0	13.3 ± 0.8
1.8	29.4 ± 1.7	9.0	22.8 ± 1.2	50.0	12.5 ± 0.8
2.0	32.7 ± 1.8	9.5	22.5 ± 1.2	60.0	12.0 ± 0.7
2.2	34.0 ± 1.9	10.0	22.1 ± 1.1	70.0	11.3 ± 0.6
2.5	35.8 ± 2.0	11.0	22.1 ± 1.2	80.0	10.8 ± 0.6
2.8	34.4 ± 2.0	12.0	20.9 ± 1.2	90.0	-
3.1	32.6 ± 2.0	13.0	20.8 ± 1.3	100	9.3 ± 0.5
3.4	29.6 ± 1.8	14.0	20.1 ± 1.1	120	-
3.7	28.3 ± 1.9	15.0	18.9 ± 1.1	150	7.8 ± 0.4
4.0	26.9 ± 1.7	16.0	18.9 ± 1.1	200	6.9 ± 0.4
4.5	25.5 ± 1.8	17.0	19.0 ± 1.1	250	6.0 ± 0.3
5.0	23.7 ± 1.8	18.0	18.2 ± 1.1	300	5.3 ± 0.3
5.5	23.8 ± 1.8	19.0	18.6 ± 1.2	350	4.9 ± 0.3
6.0	24.1 ± 2.2	20.0	17.7 ± 1.2	400	4.9 ± 0.3
6.5	24.6 ± 1.8	22.0	16.6 ± 1.0		

References

Brüche E 1929 *Ann. Phys., Lpz.* **2** 909-32
Fink M, Jost K and Herrmann D 1975 *J. Chem. Phys.* **63** 1985-7
Floeder K, Fromme D, Raith W, Schwab A and Sinapius G 1985 *J. Phys. B: At. Mol. Phys.* **18** 3347-59
Hoffman K R, Dababneh M S, Hsieh Y-F, Kauppila W E, Pol V, Smart J H and Stein T S 1982 *Phys. Rev.* A **25** 1393-403
Jain A, Tayal S S, Freitas L C G and Mu-Tao L 1983 *J. Phys. B: At. Mol. Phys.* **16** L99-106
Sueoka O 1987 *Atomic Physics with Positrons* ed J W Humberston and E A G Armour (New York: Plenum) pp 41-54
Sueoka O and Mori S 1984 *J. Phys. Soc. Japan* **53** 2491-500
—— 1986a *J. Phys. B: At. Mol. Phys.* **19** 4035-50
—— 1986b *At. Collision Res. Japan* **12** 16-17
Sueoka O, Mori S and Katayama Y 1987 *J. Phys. B: At. Mol. Phys.* **20** 3237-46
Tossell J A 1985 *J. Phys. B: At. Mol. Phys.* **18** 387-92
van Veen E H and Plantenga F L 1976 *Chem. Phys. Lett.* **38** 493-7